Publ. Astron. Soc. Japan (2014) 66 (6), 116 (1–13)
doi: 10.1093/pasj/psu108
Advance Access Publication Date: 2014 December 19

# OT J075418.7+381225 and OT J230425.8+062546: Promising candidates for the period bouncer

**Chikako NAKATA,[1,*] Taichi KATO,[1] Daisaku NOGAMI,[1] Elena P. PAVLENKO,[2,1] Tomohito OHSHIMA,[1] Enrique DE MIGUEL,[3,4] William STEIN,[5] Kazuhiko SIOKAWA,[7] Etienne MORELLE,[6] Hiroshi ITOH,[8] Pavol A. DUBOVSKY,[9] Igor KUDZEJ,[9] Hiroyuki MAEHARA,[10] Arne HENDEN,[11] William N. GOFF,[12] Shawn DVORAK,[13] Oksana I. ANTONYUK,[2] and Eddy MUYLLAERT[14]**

[1]Department of Astronomy, Kyoto University, Kitashirakawa-Oiwake-cho, Sakyo-ku, Kyoto, Kyoto 606-8502, Japan
[2]Crimean Astrophysical Observatory, 98409, Nauchny, Crimea, Ukraine
[3]Departamento de Física Aplicada, Facultad de Ciencias Experimentales, Universidad de Huelva, 21071 Huelva, Spain
[4]Center for Backyard Astrophysics, Observatorio del CIECEM, Parque Dunar, Matalascañas, 21760 Almonte, Huelva, Spain
[5]6025 Calle Paraiso, Las Cruces, NM 88012, USA
[6]9 rue Vasco de GAMA, 59553 Lauwin Planque, France
[7]810 Moriyama, Komoro, Nagano 384-0085, Japan
[8]Variable Star Observers League in Japan (VSOLJ), 1001-105 Nishiterakata-machi, Hachioji, Tokyo 192-0153, Japan
[9]Vihorlat Observatory, Mierova 4, Humenne, Slovakia
[10]Kiso Observatory, Institute of Astronomy, School of Science, The University of Tokyo, 10762-30 Mitake, Kiso-machi, Kiso-gun, Nagano 397-0101, Japan
[11]American Association of Variable Star Observers (AAVSO), 49 Bay State Rd., Cambridge, MA 02138, USA
[12]13508 Monitor Ln., Sutter Creek, CA 95685, USA
[13]Rolling Hills Observatory, 1643 Nightfall Drive, Clermont, FL 34711, USA
[14]Vereniging Voor Sterrenkunde (VVS), Moffelstraat 13, 3370 Boutersem, Belgium

*E-mail: nakata@kusastro.kyoto-u.ac.jp

Received 2014 June 6; Accepted 2014 August 31

## Abstract

We report on photometric observations of two dwarf novae, OT J075418.7+381225 and OT J230425.8+062546, which showed superoutbursts in 2013 (OT J075418) and in 2011 (OT J230425). Their mean periods of the superhump were 0.0722403(26) d (OT J075418) and 0.067317(35) d (OT J230425). These objects showed a very long growth stage of the superhump (stage A) and a large period decrease in the stage A–B transition. The long stage A suggests slow evolution of the superhump due to the very small mass ratio of these objects. The declining rates during the plateau phase in the superoutburst of these objects were lower than those of SU UMa-type dwarf novae (DNe) with a similar superhump period. These properties were similar to those of SSS J122221.7−311523, the most likely candidate for the period bouncer. Therefore, these two DNe are regarded as likely candidates for the period bouncer. We estimated the number density of period bouncers roughly from our observations for the last five years. There is a possibility that these WZ Sge-type DNe with unusual outburst properties might account for the missing population of the period bouncer suggested by the evolutionary scenario.

**Key words:** accretion, accretion disks — novae, cataclysmic variables — stars: dwarf novae — stars: individual (OT J075418.7+381225, OT J230425.8+062546)



## 1 Introduction

Cataclysmic variables (CVs) are binary star systems composed of a primary (white dwarf) and a secondary which is a typical late-type main sequence star. The secondary fills its Roche lobe and its matter spills over into the primary from the inner Lagrangian point ($L_1$ point).

Dwarf novae (DNe) are a subtype of CV. DNe show recurring outbursts. The outburst lasts days or weeks, for which their brightness increases by 2 to 5 mag. The outburst results from a release of gravitational energy which is caused by a sudden increase of the mass accretion rate by the thermal instability in the disk.

SU UMa-type dwarf novae are a subtype of DN. They have a relatively short orbital period (1–2 hr, near to the period minimum) and occasional "superoutbursts" that are brighter and have a longer duration than normal outbursts. The superhump is believed to result from the tidal instability that is triggered when the disk radius reaches the critical radius for the 3 : 1 resonance (Osaki 1989). WZ Sge-type DNe are a subgroup of SU UMa-type DN. They have a particularly short orbital period and show infrequent large-amplitude superoutbursts (for general properties of WZ Sge-type DN, see, e.g., Bailey 1979; Downes 1990; Kato et al. 2001). During the superoutburst, superhumps, periodic light variations whose periods are a few percent shorter than the orbital period, are seen. The superhump periods vary through a course of three stages: the first is stage A with a longer superhump period, the middle is stage B with a systematically varying period, and the final is stage C with a shorter superhump period (Kato et al. 2009).

According to the standard evolutionary theory of CV, the mass transfer from the secondary starts when the secondary fills its Roche lobe. The orbital period, $P_{\mathrm{orb}}$, is longer when a CV is formed, and the system develops with $P_{\mathrm{orb}}$ becoming shorter. Once its $P_{\mathrm{orb}}$ reaches the period minimum, the secondary becomes oversized for its mass as a result of deviation from thermal equilibrium or becomes a brown dwarf which cannot exist in hydrogen burning. After this point, the system evolves into a longer period and it is usually called a "period bouncer" (see, e.g., Knigge et al. 2011 and references therein, for the standard evolutionary theory of CV).

The study about the period bouncer ought to play a vital role in resolving the problems about the terminal evolution of CVs, since Kolb (1993) is said to have estimated that 70% of CVs should have passed the period bounce. The candidates for the period bouncer, however, have hardly been discovered. One of the reasons is that CVs become much fainter as they approach the period minimum (Patterson 2011). Littlefair et al. (2006) also made a great impact on the problem about the missing population in the CV. They confirmed that the secondary in the eclipsing short-period CV Sloan Digital Sky Survey (SDSS) 103533.03+055158.4 was a brown dwarf, which suggests that the system is a period bouncer. Recently, Littlefair et al. (2008) discovered three more systems which have a brown dwarf secondary with high-speed three-color photometry. Through photometric research in the period bouncer, until recently, WZ Sge-type DNe with multiple rebrightenings such as EG Cnc have been considered to be likely candidates for the period bouncer (Patterson et al. 1998). Recently, Kato and Osaki (2013) succeeded in interpreting the variation of the superhump period around stage A and developed a new dynamical method of estimating the binary's mass ratio ($q \equiv M_2/M_1$) from the stage A superhump observations and the orbital period only. By using this new method, it became evident that many of WZ Sge-type DNe with multiple rebrightenings are not likely to have such a low mass ratio as was estimated in EG Cnc (Nakata et al. 2013). After this suggestion, a new candidate for the period bouncer was discovered; Kato et al. (2013b) reported that SSS J122221.7−311523 (hereafter SSS J122221), a transient discovered by Catalina Real-time Transient Survey (CRTS: Drake et al. 2009) Siding Spring Survey (SSS), had a very small mass ratio $q = 0.045$ and a long orbital period [a possible period of 0.075879(1) d]. They also revealed a characteristic property of SSS J122221 that stage A superhumps lasted a long time.

In this paper, we present the two DNe which are similar in property to SSS J122221. OT J075418.7+381225

**Table 1.** Log of observations of OT J075418.

| Start* | End* | Mag† | Error‡ | N§ | Obs‖ | Sys# |
|---|---|---|---|---|---|---|
| 25.2913 | 25.4934 | 15.947 | 0.003 | 229 | deM | C |
| 26.2986 | 26.6882 | 16.191 | 0.010 | 489 | deM | C |
| 27.2431 | 27.6752 | 15.120 | 0.003 | 433 | MEV | C |
| 27.2980 | 27.6668 | 14.983 | 0.003 | 460 | deM | C |
| 27.6840 | 27.9237 | 14.944 | 0.003 | 286 | GFB | C |
| 28.2990 | 28.6527 | 14.923 | 0.001 | 441 | deM | C |
| 28.5383 | 28.7812 | 14.988 | 0.002 | 290 | DKS | C |
| 28.7016 | 28.9420 | 14.884 | 0.001 | 585 | SWI | *V* |
| 29.2968 | 29.6605 | 14.969 | 0.001 | 514 | deM | C |
| 29.6677 | 29.8488 | 15.019 | 0.002 | 200 | GFB | C |
| 29.7057 | 29.9564 | 14.881 | 0.001 | 609 | SWI | *V* |
| 30.2980 | 30.6371 | 15.005 | 0.001 | 500 | deM | C |
| 30.7285 | 30.9638 | 14.909 | 0.001 | 572 | SWI | *V* |
| 31.3028 | 31.6423 | 15.050 | 0.001 | 502 | deM | C |
| 31.7016 | 31.9142 | 14.968 | 0.001 | 364 | SWI | *V* |
| 32.3015 | 32.6886 | 15.105 | 0.001 | 608 | deM | C |
| 32.3054 | 32.6595 | 15.138 | 0.001 | 355 | MEV | C |
| 33.3011 | 33.6583 | 15.175 | 0.001 | 354 | MEV | C |
| 36.5681 | 36.5681 | 15.180 | — | 1 | MUY | C |
| 36.6996 | 36.9058 | 1.169 | 0.001 | 353 | SWI | C |
| 36.6996 | 36.9058 | 15.198 | 0.001 | 353 | SWI | *V* |
| 37.6966 | 37.8978 | 1.166 | 0.001 | 345 | SWI | C |
| 38.3036 | 38.6830 | 15.270 | 0.001 | 468 | CDZ | C |
| 39.3021 | 39.5805 | 15.299 | 0.002 | 308 | CDZ | C |
| 39.3564 | 39.6420 | 15.347 | 0.001 | 256 | MEV | C |
| 40.3004 | 40.6396 | 15.386 | 0.002 | 251 | MEV | C |
| 40.3940 | 40.6534 | 15.346 | 0.002 | 293 | CDZ | C |
| 46.3199 | 46.4654 | 15.350 | 0.003 | 148 | MEV | C |
| 47.4372 | 47.6331 | 15.362 | 0.002 | 207 | deM | C |
| 48.4312 | 48.6151 | 15.415 | 0.002 | 232 | deM | C |
| 49.4269 | 49.6170 | 15.449 | 0.003 | 212 | deM | C |
| 50.4413 | 50.5910 | 15.499 | 0.002 | 182 | deM | C |
| 52.2781 | 52.5203 | 2.233 | 0.005 | 281 | DPV | C |
| 53.3085 | 53.5875 | 15.658 | 0.002 | 354 | deM | C |
| 54.2581 | 54.4964 | 2.554 | 0.003 | 300 | DPV | C |
| 54.3650 | 54.6011 | 15.740 | 0.002 | 184 | MEV | C |
| 56.2530 | 56.5597 | 2.655 | 0.002 | 386 | DPV | C |
| 57.2314 | 57.5306 | 2.781 | 0.002 | 360 | DPV | C |

*BJD−2456300.0.
†Mean magnitude.
‡1 $\sigma$ of the mean magnitude.
§Number of observations.
‖Observer's code: deM (E. de Miguel), MEV (E. Morelle), GFB (W. N. Goff), DKS (S. Dvorak), SWI (W. Stein), MUY (E. Muyllaert), CDZ (AAVSO data), and DPV (P. A. Dubovsky).
#Filter. "*V*" means *V* filter and "C" means no filter (clear).

**Table 2.** Log of observations of OT J230425.

| Start* | End* | Mag† | Error‡ | N§ | Obs‖ | Sys# |
|---|---|---|---|---|---|---|
| 63.9532 | 64.0147 | 13.775 | 0.005 | 130 | Siz | C |
| 65.8770 | 65.9577 | 14.149 | 0.004 | 146 | Mhh | C |
| 65.8827 | 65.9319 | 13.683 | 0.005 | 107 | Ioh | C |
| 65.8902 | 66.0023 | 13.783 | 0.002 | 224 | Siz | C |
| 67.8853 | 68.0198 | 13.871 | 0.005 | 264 | Siz | C |
| 68.8860 | 69.0162 | 13.876 | 0.004 | 259 | Siz | C |
| 68.9449 | 69.0041 | 13.887 | 0.008 | 132 | Ioh | C |
| 68.9769 | 68.9841 | 14.259 | 0.019 | 16 | Mhh | C |
| 69.8702 | 70.0000 | 13.879 | 0.006 | 280 | Ioh | C |
| 69.8802 | 69.9934 | 14.217 | 0.004 | 424 | Mhh | C |
| 69.8892 | 70.0194 | 13.918 | 0.007 | 231 | Siz | C |
| 70.8707 | 71.0046 | 13.908 | 0.007 | 268 | Ioh | C |
| 71.8613 | 71.9994 | 13.851 | 0.005 | 292 | Ioh | C |
| 71.8624 | 72.0124 | 13.848 | 0.006 | 299 | Siz | C |
| 72.1643 | 72.2480 | 14.044 | 0.022 | 29 | CRI | C |
| 73.1712 | 73.2678 | 13.813 | 0.008 | 47 | CRI | C |
| 73.9053 | 73.9859 | 14.018 | 0.016 | 132 | Ioh | C |
| 73.9302 | 74.0088 | 14.028 | 0.016 | 120 | Siz | C |
| 74.8823 | 74.9998 | 13.951 | 0.009 | 236 | Siz | C |
| 75.1832 | 75.2627 | 13.920 | 0.012 | 26 | CRI | C |
| 75.8838 | 75.9353 | 14.272 | 0.009 | 182 | Mhh | C |
| 75.9042 | 75.9720 | 13.962 | 0.006 | 134 | Siz | C |
| 78.8920 | 78.9520 | 14.094 | 0.007 | 122 | Siz | C |
| 78.9242 | 78.9722 | 14.508 | 0.008 | 182 | Mhh | C |
| 79.9057 | 79.9786 | 14.275 | 0.015 | 120 | Siz | C |
| 80.8940 | 80.9777 | 14.449 | 0.022 | 166 | Siz | C |
| 80.9083 | 80.9452 | 14.588 | 0.009 | 136 | Mhh | C |
| 83.8728 | 83.9645 | 14.549 | 0.016 | 158 | Ioh | C |
| 86.9111 | 86.9111 | 17.401 | — | 1 | Siz | C |

*BJD−2455500.0.
†Mean magnitude.
‡1 $\sigma$ of the mean magnitude.
§Number of observations.
‖Observer's code: Siz (K. Shiokawa), Mhh (H. Maehara), Ioh (H. Itoh), and CRI (Crimean Astrophys. Obs.).
#Filter. "C" means no filter (clear).

(hereafter OT J075418) was detected by CRTS to be CSS 130131:075419+381225 on 2013 January 31. The quiescent counterpart was $g = 22.8$ mag SDSS J075418.72+381225.2. The observed superhumps with a period of 0.07 d suggested an SU UMa-type dwarf nova (vsnet-alert 15355). OT J230425.8+062546 (hereafter OT J230425) was originally reported that it was discovered to be a possible nova by H. Nishimura on 2010 December 29 at 13.7 mag (Nakano et al. 2011). The quiescent counterpart was $g = 21.1$ mag SDSS J230425.88+062545.6. After that, it was suggested that the nova was a dwarf nova on the basis of the color of the SDSS counterpart (vsnet-alert 12548). From subsequent observations the presence of superhumps with an amplitude of 0.06 mag was detected (A. Arai, vsnet-alert 12563). Although observations and analysis of OT J230425 were already reported in a summary form in Kato et al. (2012), we present a new interpretation of this object in this paper.

This paper is structured as follows. Section 2 briefly shows a log of observations and our analysis method. Sections 3 and 4 deal with the results of the observations of OT J075418 and OT J230425, respectively. In section 5 we discuss the results.

## 2 Observation and analysis

Tables 1 and 2 show the logs of photometric observations. All the observation times were written in barycentric Julian date (BJD). To correct zero-point of data differences between different observers, we added a constant to each observer's data.

The phase dispersion minimization (PDM) method (Stellingwerf 1978) was used for a period analysis. In subtracting the global trend of the light curve, we subtracted a smoothed light curve obtained by locally weighted polynomial regression (LOWESS: Cleveland 1979) before making the PDM analysis. The 1 $\sigma$ error of the best estimated period by the PDM analysis was determined by the methods in Fernie (1989) and Kato et al. (2010).

A variety of bootstraps was used for estimating the robustness of the result of PDM. We analyzed about 100 samples which randomly contained 50% of observations, and performed a PDM analysis for these samples. The result of the bootstrap is shown as a form of 90% confidence intervals in the resultant $\theta$ statistics.

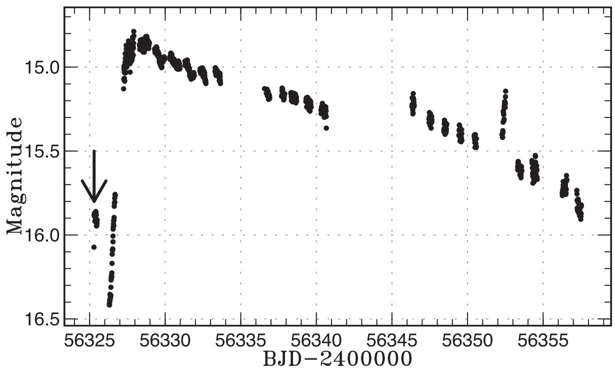


**Fig. 1.** Overall light curve of OT J075418. The data were binned to 0.01 d. The arrow indicates a precursor.

## 3 OT J075418.7+381225

### 3.1 Overall light curve

In figure 1 is shown the overall light curve of OT J075418. After a precursor outburst (marked with an arrow in figure 1), the superoutburst began on BJD 2456326. The early rise was well observed during BJD 2456326–2456327. The superoutburst lasted with a slow decline for at least 30 d. In the middle part of the superoutburst (BJD 2456341–2456345), there were no observations. On BJD 2456346, observations were resumed, and they showed

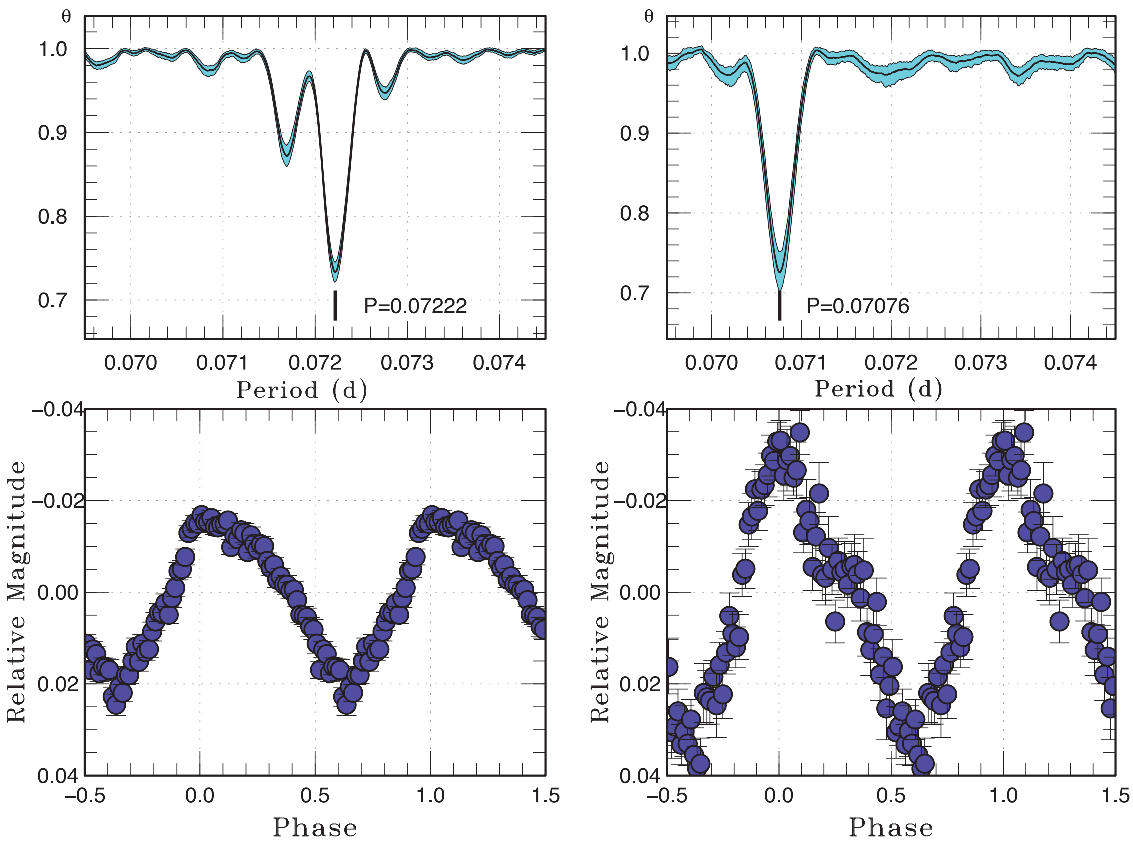


**Fig. 2.** Superhumps in OT J075418 (BJD 2456328–2456358). Left-hand upper: $\theta$ diagram of our PDM analysis of stage A superhumps (BJD 2456328–2456341). Left-hand lower: Phase-averaged profile of stage A superhumps. Right-hand upper: $\theta$ diagram of our PDM analysis of stage B superhumps (BJD 2456345–2456355). Right-hand lower: Phase-averaged profile of stage B superhumps. (Color online)

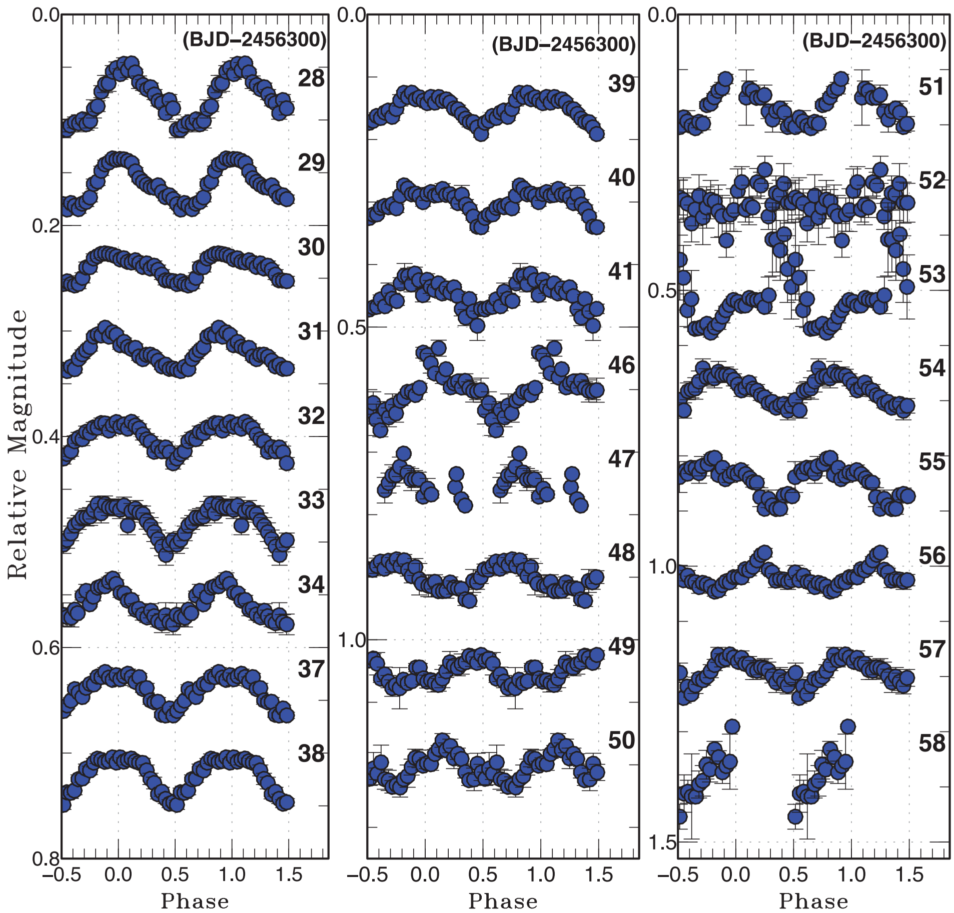


**Fig. 3.** Nightly variation of the profile of superhumps in OT J075418. (Color online)

a small rise in brightness. On BJD 2456352, there was a rapid brightening. This phenomenon was confirmed by using different comparison stars. It may have been the interesting phenomenon that we could not explain theoretically. However, it may have been an artifact, because the observing condition was very bad due to clouds and the Moon.

## 3.2 Superhumps

In figure 2, a period analysis by using the Phase Dispersion Minimization method (PDM: Stellingwerf 1978) indicated the presence of periods of 0.072218(3) d during stage A (BJD 2456328–2456341) and 0.070758(6) d during stage B (BJD 2456345–2456355). The mean profiles of stage A and stage B superhumps are also shown in the lower panels of figure 2. The amplitude of the superhumps during stage B is larger than that during stage A.

In figure 3 is shown the nightly variation of the profile of superhumps. The amplitude of superhumps was 0.03–0.06 mag, smaller than those in typical SU UMa-type DNe.

We determined the times of maxima of ordinary superhumps in the same way as in Kato et al. (2009). The resultant times are listed in table 3.

The $O-C$ curve of OT J075418 is shown in figure 4. The very long stage A ($30 \le E \le 220$) and stage B ($E \ge 280$) are seen. Although the data when the stage A–B transition took place cannot be estimated precisely because of lack of observations, it occurred between BJD 2456342 and 2456346. In stage A, superhumps with a mean period of $P_{\rm sh} = 0.0722179(32)$ d and the time derivative of the superhump period $P_{\rm dot}$ $(= \dot{P}/P) = +3.6(0.7) \times 10^{-5}$ s s$^{-1}$ were recorded. In stage B, superhumps with a mean period of 0.0707581(58) d and $P_{\rm dot}$ of $-2.4(0.5) \times 10^{-5}$ s s$^{-1}$ were recorded.

## 3.3 Two-dimensional Lasso analysis

The least absolute shrinkage and selection operator (Lasso) method was introduced by Kato and Uemura (2012). This method has been proven very effective in separating closely spaced periods and has been extended

**Table 3.** Times of superhump maxima in OT J075418.

| *E* | Max* | Error | *O* – *C*† | *N*‡ |
|---|---|---|---|---|
| 0 | 56325.4119 | 0.0040 | – 0.0295 | 65 |
| 13 | 56326.3502 | 0.0065 | – 0.0224 | 72 |
| 14 | 56326.4264 | 0.0018 | – 0.0179 | 73 |
| 15 | 56326.4975 | 0.0013 | – 0.0184 | 71 |
| 16 | 56326.5656 | 0.0019 | – 0.0219 | 72 |
| 17 | 56326.6432 | 0.0020 | – 0.0160 | 74 |
| 26 | 56327.2791 | 0.0005 | – 0.0249 | 64 |
| 27 | 56327.3527 | 0.0005 | – 0.0229 | 136 |
| 28 | 56327.4234 | 0.0004 | – 0.0238 | 138 |
| 29 | 56327.4965 | 0.0008 | – 0.0224 | 125 |
| 30 | 56327.5678 | 0.0004 | – 0.0227 | 106 |
| 31 | 56327.6370 | 0.0005 | – 0.0251 | 139 |
| 32 | 56327.7092 | 0.0004 | – 0.0246 | 62 |
| 33 | 56327.7832 | 0.0010 | – 0.0222 | 64 |
| 34 | 56327.8537 | 0.0007 | – 0.0233 | 71 |
| 35 | 56327.9219 | 0.0023 | – 0.0268 | 44 |
| 41 | 56328.3564 | 0.0007 | – 0.0221 | 73 |
| 42 | 56328.4308 | 0.0007 | – 0.0193 | 73 |
| 43 | 56328.4955 | 0.0009 | – 0.0263 | 71 |
| 44 | 56328.5700 | 0.0008 | – 0.0234 | 138 |
| 45 | 56328.6443 | 0.0011 | – 0.0208 | 123 |
| 46 | 56328.7130 | 0.0010 | – 0.0236 | 157 |
| 47 | 56328.7840 | 0.0005 | – 0.0243 | 178 |
| 48 | 56328.8524 | 0.0006 | – 0.0275 | 141 |
| 49 | 56328.9284 | 0.0010 | – 0.0232 | 115 |
| 55 | 56329.3637 | 0.0029 | – 0.0177 | 87 |
| 56 | 56329.4315 | 0.0012 | – 0.0216 | 83 |
| 57 | 56329.5031 | 0.0023 | – 0.0215 | 82 |
| 58 | 56329.5719 | 0.0013 | – 0.0244 | 83 |
| 59 | 56329.6463 | 0.0016 | – 0.0216 | 61 |
| 60 | 56329.7189 | 0.0007 | – 0.0207 | 158 |
| 61 | 56329.7986 | 0.0014 | – 0.0126 | 198 |
| 62 | 56329.8692 | 0.0013 | – 0.0137 | 157 |
| 63 | 56329.9355 | 0.0017 | – 0.0190 | 133 |
| 69 | 56330.3692 | 0.0015 | – 0.0151 | 85 |
| 70 | 56330.4385 | 0.0011 | – 0.0174 | 84 |
| 71 | 56330.5183 | 0.0014 | – 0.0092 | 86 |
| 72 | 56330.5836 | 0.0010 | – 0.0156 | 89 |
| 74 | 56330.7380 | 0.0024 | – 0.0045 | 78 |
| 75 | 56330.8028 | 0.0009 | – 0.0113 | 140 |
| 76 | 56330.8767 | 0.0007 | – 0.0091 | 141 |
| 77 | 56330.9376 | 0.0011 | – 0.0198 | 141 |
| 83 | 56331.3822 | 0.0019 | – 0.0050 | 80 |
| 84 | 56331.4572 | 0.0011 | – 0.0017 | 77 |
| 85 | 56331.5234 | 0.0014 | – 0.0071 | 95 |
| 86 | 56331.5895 | 0.0028 | – 0.0126 | 94 |
| 88 | 56331.7528 | 0.0020 | 0.0074 | 99 |
| 89 | 56331.8094 | 0.0018 | – 0.0077 | 99 |
| 90 | 56331.8869 | 0.0022 | – 0.0018 | 99 |
| 97 | 56332.4002 | 0.0027 | 0.0100 | 158 |
| 97 | 56332.4002 | 0.0027 | 0.0100 | 158 |
| 98 | 56332.4612 | 0.0018 | – 0.0006 | 145 |
| 99 | 56332.5408 | 0.0021 | 0.0074 | 154 |
| 100 | 56332.6046 | 0.0018 | – 0.0004 | 152 |

**Table 3.** (Continued)

| *E* | Max* | Error | *O* – *C*† | *N*‡ |
|---|---|---|---|---|
| 101 | 56332.6660 | 0.0058 | – 0.0107 | 127 |
| 110 | 56333.3244 | 0.0012 | 0.0030 | 45 |
| 111 | 56333.3999 | 0.0008 | 0.0068 | 59 |
| 112 | 56333.4755 | 0.0022 | 0.0108 | 61 |
| 113 | 56333.5443 | 0.0027 | 0.0080 | 54 |
| 114 | 56333.6192 | 0.0008 | 0.0112 | 61 |
| 157 | 56336.7342 | 0.0008 | 0.0459 | 188 |
| 158 | 56336.7965 | 0.0006 | 0.0365 | 198 |
| 159 | 56336.8676 | 0.0013 | 0.0359 | 196 |
| 171 | 56337.7416 | 0.0011 | 0.0504 | 99 |
| 172 | 56337.8029 | 0.0012 | 0.0400 | 99 |
| 179 | 56338.3237 | 0.0015 | 0.0593 | 51 |
| 180 | 56338.3865 | 0.0013 | 0.0505 | 71 |
| 181 | 56338.4648 | 0.0013 | 0.0572 | 70 |
| 182 | 56338.5365 | 0.0010 | 0.0572 | 71 |
| 183 | 56338.6070 | 0.0018 | 0.0561 | 72 |
| 193 | 56339.3314 | 0.0025 | 0.0641 | 74 |
| 194 | 56339.4109 | 0.0011 | 0.0720 | 73 |
| 195 | 56339.4686 | 0.0017 | 0.0580 | 131 |
| 196 | 56339.5543 | 0.0045 | 0.0721 | 136 |
| 197 | 56339.6130 | 0.0009 | 0.0592 | 69 |
| 207 | 56340.3481 | 0.0020 | 0.0779 | 55 |
| 208 | 56340.4063 | 0.0029 | 0.0645 | 91 |
| 209 | 56340.4856 | 0.0013 | 0.0722 | 123 |
| 210 | 56340.5570 | 0.0020 | 0.0719 | 89 |
| 211 | 56340.6249 | 0.0013 | 0.0681 | 91 |
| 291 | 56346.3452 | 0.0008 | 0.0575 | 47 |
| 292 | 56346.4170 | 0.0007 | 0.0576 | 56 |
| 307 | 56347.4816 | 0.0011 | 0.0478 | 50 |
| 308 | 56347.5504 | 0.0015 | 0.0449 | 61 |
| 309 | 56347.6214 | 0.0020 | 0.0442 | 49 |
| 321 | 56348.4747 | 0.0011 | 0.0379 | 71 |
| 322 | 56348.5453 | 0.0018 | 0.0368 | 70 |
| 335 | 56349.4669 | 0.0012 | 0.0272 | 70 |
| 336 | 56349.5385 | 0.0013 | 0.0272 | 46 |
| 337 | 56349.6049 | 0.0017 | 0.0220 | 59 |
| 376 | 56352.3683 | 0.0014 | – 0.0085 | 70 |
| 390 | 56353.3551 | 0.0011 | – 0.0246 | 72 |
| 391 | 56353.4255 | 0.0011 | – 0.0258 | 70 |
| 392 | 56353.4981 | 0.0012 | – 0.0249 | 72 |
| 393 | 56353.5691 | 0.0010 | – 0.0256 | 63 |
| 404 | 56354.3470 | 0.0012 | – 0.0357 | 74 |
| 405 | 56354.4204 | 0.0021 | – 0.0339 | 99 |
| 406 | 56354.4874 | 0.0009 | – 0.0385 | 105 |
| 407 | 56354.5571 | 0.0010 | – 0.0404 | 55 |
| 432 | 56356.3251 | 0.0020 | – 0.0633 | 71 |
| 433 | 56356.3984 | 0.0031 | – 0.0617 | 72 |
| 434 | 56356.4674 | 0.0014 | – 0.0643 | 70 |
| 435 | 56356.5428 | 0.0012 | – 0.0606 | 61 |
| 446 | 56357.3150 | 0.0016 | – 0.0764 | 67 |
| 447 | 56357.3838 | 0.0018 | – 0.0793 | 67 |
| 448 | 56357.4591 | 0.0013 | – 0.0756 | 70 |

*BJD−2400000.0.
†$C = 2456325.4414 + 0.0716368\,E$.
‡Number of points used for determining the maximum.

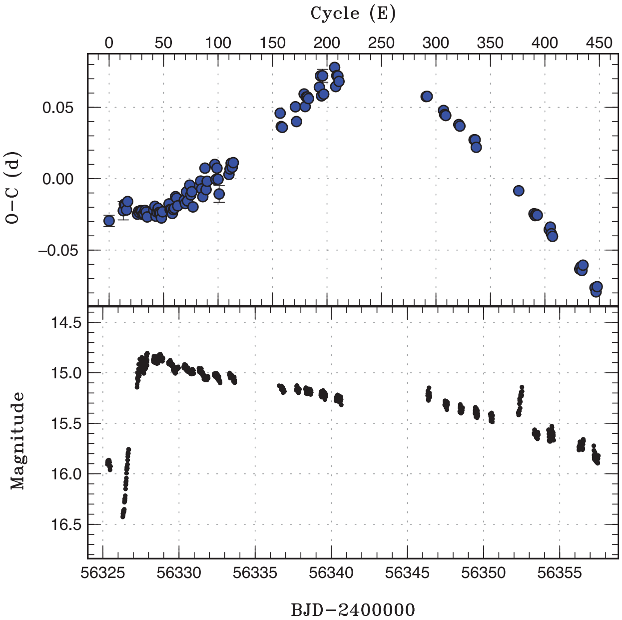


**Fig. 4.** Upper: The $O-C$ curve of OT J075418. An ephemeris of BJD 2456325.4414+0.0716368$E$ was used for drawing this figure. Lower: Overall light curve, the same as figure 1. The horizontal axis in units of BJD and cycle number is common to both of upper and lower panels. (Color online)

to two-dimentional power spectra (Osaki & Kato 2013; Kato & Maehara 2013).

A two-dimensional Lasso analysis of OT J075418 data is shown in figure 5. A major change in frequency from ∼ 13.85 cycles/day (c/d) to ∼ 14.1 c/d can be seen between BJD 2456341 and 2456345. It suggests that the change took place with good timing when the stage A–B transition occurred. During stage A (BJD 2456328–2456341), the frequency becomes lower. In contrast, it shows a tendency to become higher in stage B (BJD 2456345–2456355).

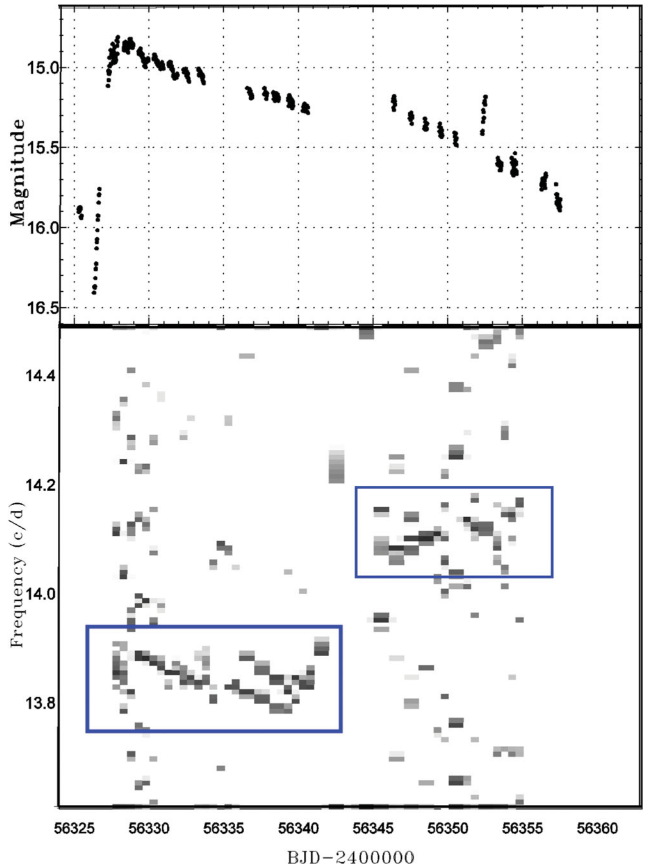


**Fig. 5.** Two-dimensional Lasso period analysis of OT J075418. Upper: Overall light curve binned to 0.01 d, the same as figure 1. Lower: Result of two-dimensional Lasso analysis (5 d window, 0.5 d shift, and log $\lambda$ = −8.5). The appearances of the stage A and stage B frequencies are boxed. (Color online)

## 4 OT J230425.8+062546

### 4.1 Overall light curve

In figure 6 is shown the overall light curve of OT J230425. This object was discovered on 2010 December 29 (JD 2455559) with a recordable possible maximum brightness of $V = 13.72$. The early rise was missed. The superoutburst lasted ∼ 25 d. The light curve showed a slow decline until BJD 2455575. After BJD 2455578, it declined faster.

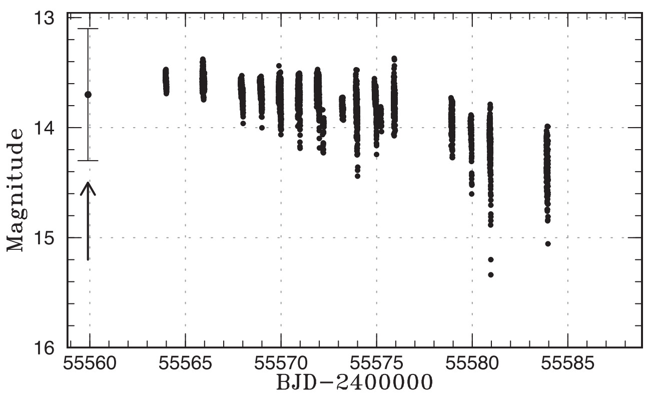


**Fig. 6.** Overall light curve of OT J230425. The data were binned to 0.01 d. The arrow indicates the discovery of the superoutburst (Nakano et al. 2011).

### 4.2 Superhumps

During BJD 2455563–2455585, superhumps with an amplitude of 0.03–0.07 mag were present. A period analysis by using all the data indicated that the mean superhump period was 0.067317(35) d. The PDM analysis of all superhumps was described in Kato et al. (2012).

A period analysis indicated a change in period from 0.067245(17) d during stage A (BJD 2455563–2455572) to 0.066351(12) d during stage B (BJD 2455571–2455585) (figure 7). The mean profiles of stage A and stage B superhumps are also shown in the lower panels of figure 7. In

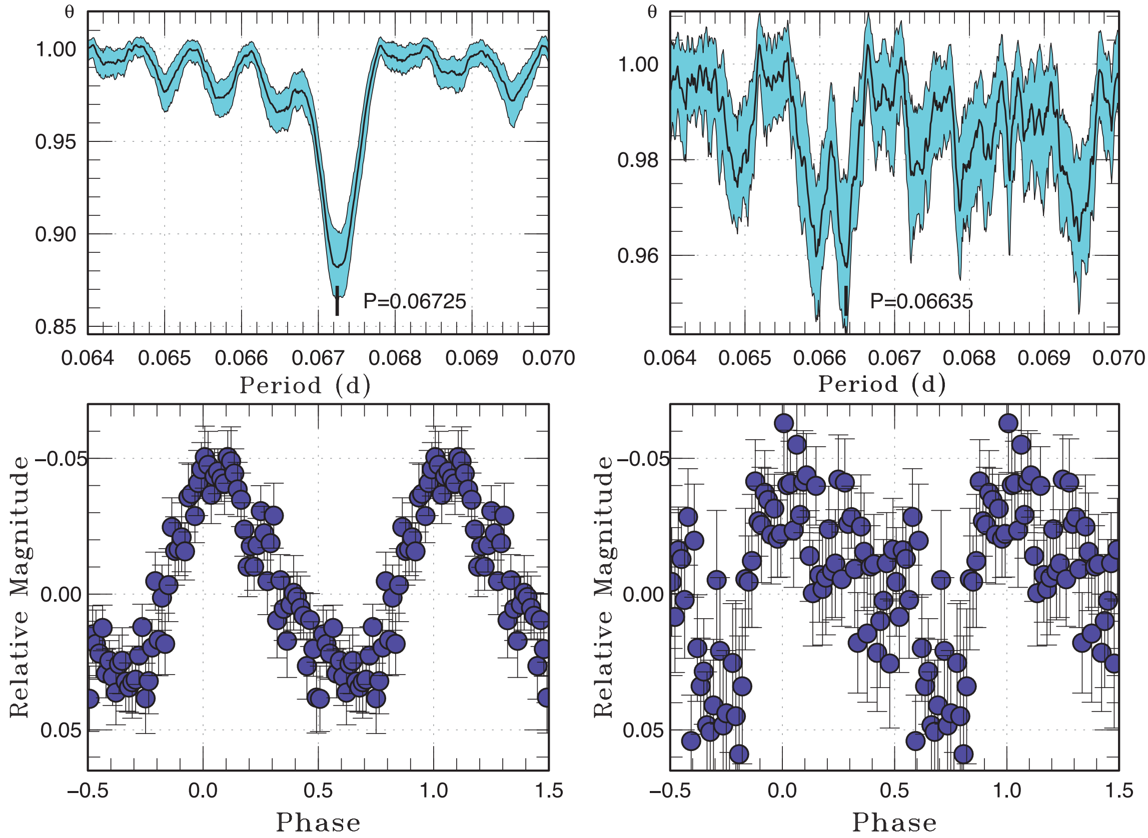


**Fig. 7.** Superhumps in OT J230425 (BJD 2455563–2455585). Left-hand upper: $\theta$ diagram of our PDM analysis of stage A superhumps (BJD 2455563–2455572). Left-hand lower: Phase-averaged profile of stage A superhumps. Right-hand upper: $\theta$ diagram of our PDM analysis of stage B superhumps (BJD 2455571–2455585). Right-hand lower: Phase-averaged profile of stage B superhumps. (Color online)

figure 8 is shown the nightly variation of the profile of superhumps. The maximum amplitude of superhumps was seen around BJD 2455571.

As shown in the right-hand upper panel of figure 7, there was a possible period which is shorter than the indicated period 0.066351(12) d. It was suggested that the period was a possible orbital period of 0.06589(1) d. Assuming 0.06589(1) d to be the orbital period, the new method of estimating the binary's mass ratio, $q$, by using stage A superhumps (Kato & Osaki 2013) implies $q = 0.053(1)$. It suggests that OT J230425 is a likely candidate for the period bouncer.

In figure 9 is described an $O - C$ curve of OT J230425 (filled circles), compared with $O - C$ curve of OT J075418 exhibited in figure 4 (filled squares). The resultant times of OT J230425 are listed in table 4. The $O - C$ curve of OT J230425 is very similar to that of OT J075418. The very long stage A ($E \leq 123$) and the subsequent stage B ($E \geq 118$) are seen. The stage A–B transition occurred around BJD 2455572. The periods of superhumps in stage A and stage B were 0.067194(30) d and 0.066281(63) d, respectively. The $P_{\mathrm{dot}}$ in stage B was $-3.9(2.4) \times 10^{-5}\,\mathrm{s\,s^{-1}}$.

## 5 Discussion

### 5.1 Decrease of superhump period between stage A and stage B

The $O - C$ curves of OT J075418 and OT J230425 (figures 4 and 9) suggest a very long stage of increasing $O - C$ values (or a long period) and a certain stage transition in the middle of the superoutbursts. Kato et al. (2009) argued that the superhump period usually decreases by 1.0%–1.5% at the stage A–B transition and by $\sim$0.5% at the stage B–C transition. The fractional period decreases at the transition were $\sim$2.0% in OT J075418 and $\sim$1.4% in OT J230425. Such a large variation in frequency of OT J075418 can be clearly seen in figure 5. Since they were too large for a stage B–C transition, we regard this transition as a stage A–B transition.

The disk precession results mainly from direct axisymmetric tidal potential of the secondary, secondarily from the gas pressure in the eccentric mode and resonant wave stress (Lubow 1992). Although the tidal potential produces a net prograde precession, the gas pressure effect makes a retrograde contribution and decreases the precession rate. Murray (2000) gave the hydrodynamical precession $\omega$ in

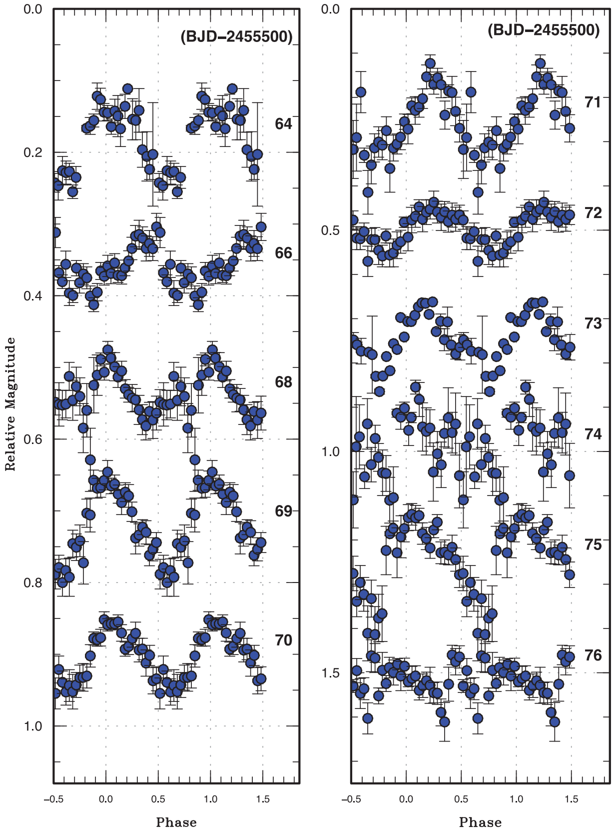


**Fig. 8.** Nightly variations of the profile of superhumps in OT J230425. (Color online)

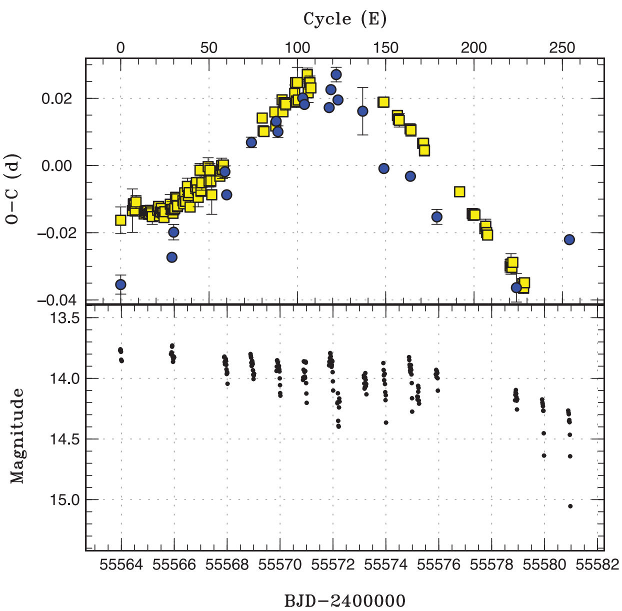


**Fig. 9.** Upper: $O-C$ curve of OT J230425, compared with that of OT J075418. Filled circles and filled squares represent $O-C$ diagrams of OT J230425 and OT J075418, respectively. The $O-C$ diagram of OT J075418 was shifted to fit it to that of OT J230425 . An ephemeris of BJD 2455565.925 + 0.06695$E$ was used for drawing this figure. Lower: Light curve of OT J230425, the same as figure 6 except its leftmost part. (Color online)

**Table 4.** Times of superhump maxima in OT J230425.

| $E$ | Max* | Error | $O-C$† | $N$‡ |
|---|---|---|---|---|
| 0 | 55563.9791 | 0.0028 | −0.0354 | 108 |
| 29 | 55565.9214 | 0.0011 | −0.0273 | 274 |
| 30 | 55565.9956 | 0.0023 | −0.0198 | 64 |
| 59 | 55567.9479 | 0.0017 | −0.0019 | 104 |
| 60 | 55568.0077 | 0.0015 | −0.0087 | 70 |
| 74 | 55568.9571 | 0.0016 | 0.0069 | 215 |
| 88 | 55569.8972 | 0.0014 | 0.0132 | 347 |
| 89 | 55569.9608 | 0.0018 | 0.0101 | 427 |
| 103 | 55570.9046 | 0.0013 | 0.0201 | 116 |
| 104 | 55570.9694 | 0.0011 | 0.0182 | 107 |
| 118 | 55571.9022 | 0.0009 | 0.0172 | 217 |
| 119 | 55571.9743 | 0.0014 | 0.0226 | 211 |
| 122 | 55572.1788 | 0.0022 | 0.0271 | 15 |
| 123 | 55572.2380 | 0.0014 | 0.0195 | 12 |
| 137 | 55573.1684 | 0.0071 | 0.0162 | 16 |
| 149 | 55573.9517 | 0.0014 | −0.0009 | 148 |
| 164 | 55574.9499 | 0.0013 | −0.0032 | 107 |
| 179 | 55575.9383 | 0.0022 | −0.0153 | 150 |
| 224 | 55578.9187 | 0.0043 | −0.0364 | 237 |
| 254 | 55580.9340 | 0.0014 | −0.0221 | 192 |

*BJD−2400000.0.
†$C = 2455565.925 + 0.06695\,E$.
‡Number of points used for determining the maximum.

terms of the dynamic precession ($\omega_{\rm dyn}$) and the pressure contribution to the precession ($\omega_{\rm pres}$):

$$\omega = \omega_{\rm dyn} + \omega_{\rm pres}. \qquad (1)$$

Note that $\omega_{\rm pres}$ is a negative value according to its retrograde contribution. The ratio $\omega_{\rm pres}/\omega_{\rm orb}$ corresponds to the fractional decrease of the superhump period in transition between stage A and stage B, where $\omega_{\rm orb}$ is the orbital frequency. Therefore, it is possible that the large decrease in superhump period between stage A and stage B indicates a large pressure contribution.

## 5.2 Slow evolution of superhumps

The duration of stage A reflects the growth time of the 3 : 1 resonance. As described in subsections 3.2 and 4.2, it took ∼190 superhump cycles (OT J075418) and ∼120 (OT J230425) to fully develop into the 3 : 1 resonance. Considering the absence of observations immediately after the discovery of OT J230425, the growth time of the 3 : 1 resonance may be even longer in OT J230425. This long duration of stage A suggests very small mass ratios $q$ of these objects because the growth time of the 3 : 1 resonance is expected to be inversely proportional to $q^2$ (Lubow 1991). The duration of stage A of these objects was 4–8 times longer than those of typical SU UMa-type DNe with a short orbital period of $\sim 0.06$ d and a mass ratio of 0.10–0.15 (Kato et al. 2009). The mass ratio of these objects can be estimated to be 2–3 times smaller, suggesting a possible mass ratio $\sim 0.05$. Despite the possible very small mass ratios, the orbital period of these objects, which are estimated to be less than 1% shorter than their superhump periods, are longer than that of a typical short-period SU UMa ($P_{\mathrm{orb}} \sim 0.06$ d). This supports the hypothesis that these objects are candidates for the period bouncer.

## 5.3 Slow fading rate

During the superoutburst of SU UMa-type dwarf novae, an almost exponential, slow-declining phase exists, which is called the plateau phase. Osaki (1989) derived the time scale of this slow fading as follows:

$$t_{\mathrm{d}} \simeq 8.14 R_{\mathrm{d},10}^{0.4} \alpha_{0.3}^{-0.7} [\mathrm{d}], \qquad (2)$$

where $R_{\mathrm{d},10}$ is the disk radius in units of $10^{10}$ cm and $\alpha_{0.3}$ is $\alpha_{\mathrm{hot}}/0.3$ ($\alpha_{\mathrm{hot}}$ represents the disk viscosity in the hot state). Kato et al. (2014a) suggested that $\alpha_{\mathrm{hot}}$ in the candidate for the period bouncer that show slow fading rate is probably smaller than in higher-$q$ systems. In addition to this, the radius of the 3 : 1 resonance can be formulated in terms of $q$:

$$r_{3:1} = 3^{(-2/3)}(1+q)^{-1/3}. \qquad (3)$$

Thus a small $q$ produces a large radius of the 3 : 1 resonance and a large disk radius. But the contribution by a small $q$ is smaller than that by a small $\alpha_{\mathrm{hot}}$, since equation (2) shows the dependence of $t_{\mathrm{d}}$ on $q$ is larger than that on $\alpha$.

The fading rates of OT J075418 and OT J230425 were 0.0189(3) mag $\mathrm{d}^{-1}$ and 0.0340(4) mag $\mathrm{d}^{-1}$, respectively. In figure 10 is shown the relation between the superhump period in stage B ($P_{\mathrm{orb}}$) and the fading rate of SU UMa-type DNe (filled circles), WZ Sge-type DNe (filled triangles), and possible candidates for the period bouncer including OT J075418 and OT J230425 (filled stars). SSS J122221 (J122221 in figure 10) was reported as a perfect candidate for the period bouncer (Kato et al. 2013b). Kato et al. (2013b) also suggests that OT J184228.1+483742 (J184228 in figure 10) showing a double superoutburst is a likely candidate for the period bouncer. In figure 10, the fading rates of OT J075418 and OT J230418 are lower than those of SU UMa-type DNe with a similar period. Furthermore, the location of these objects

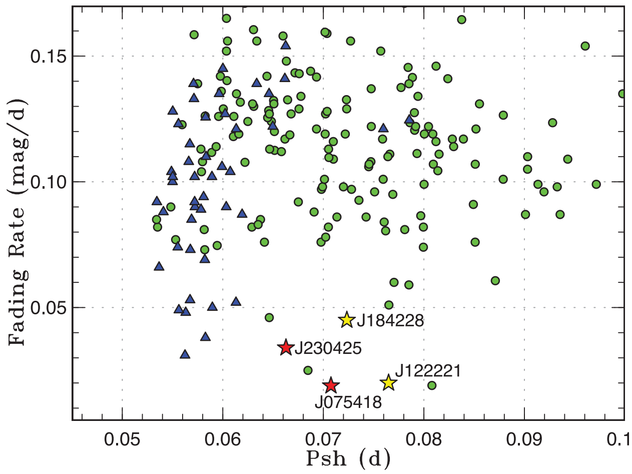


**Fig. 10.** Fading rate versus superhump period in stage B. The data are obtained from Kato et al. (2014a). The filled circles and the filled triangles represent SU UMa-type DNe and WZ Sge-type DNe, respectively. The filled stars represent the candidates for the period bouncer, including OT J075418 and OT J230425. (Color online)

is close to that of the likely candidates previously suggested for the period bouncer. This increases the possibility that these two objects are likely candidates for the period bouncer.

There are two more objects near these candidates for the period bouncer in figure 10. One of them is BC Dor, which showd a superoutburst in 2003, and another is PV Per detected in its superoutburst in 2008. Their last superoutbursts were reported in Kato et al. (2009). Since they had relatively frequent outbursts, we considered them not to be candidates for the period bouncer. They were within a range of the period bouncer including errors due to the poor-quality data in figure 10.

## 5.4 Absence of early superhumps

OT J184228, a likely candidate for the period bouncer, showed a double superoutburst consisting of the first one with early superhumps and another with ordinary superhumps (Kato et al. 2013b). SSS J122221 also showed a similar pattern to the superoutburst.

OT J075418 and OT J230425, however, showed no early superhumps. Early superhumps, as mentioned in section 1, arise when the disk radius reaches the 2:1 resonance radius due to its low $q$. And they cannot be detected in a system with a low inclination (e.g., GW Lib reported by Hiroi et al. 2009), since the origin of early superhumps is the emission of a disk surface that has a nonaxisymmetric vertical structure (Nogami et al. 1997; Kato 2002). The absence of the stage of early superhumps may indicate that the radius of the 2 : 1 resonance was not reached by the disk radius of these objects. Although this does not generally support their low $q$'s, we expect OT J075418 and

OT J230425 to have a low $q$ because of other strong evidence that we discussed above. Furthermore, it has been reported that a system with a low $q$ corroborated did not show early superhumps (Kato et al. 2014b). It was considered that the superoutburst triggered by an inside-out (slowly rising) outburst made it impossible to establish the 2 : 1 resonance.

## 5.5 Existence of a precursor in OT J075418

In OT J075418, a precursor preceding its superoutburst was detected (BJD 2456325). This is rare for a WZ Sge-type DN, which hardly shows the normal outburst.

Osaki and Meyer (2003) suggested that in a superoutburst with a precursor the disk radius does not reach the tidal truncation radius, which is the maximum radius and larger than the 3 : 1 resonance one, while the disk radius reaches the tidal truncation radius in a superoutburst without a precursor. It is thought that the system in a precursor fades rapidly the same as in a normal outburst, since its accretion disk does not reach the tidal truncation radius and the disk permits the cooling wave to propagate inwardly. During this fading, if the disk becomes sufficiently eccentric, the tidal dissipation from the secondary brings the disk to the hot state. Then, we observe that it is a superoutburst with a precursor. As mentioned in subsection 5.3, however, OT J075418 faded very slowly. Similarly, 1RXS J053234+624755 has a very small mass ratio, 0.074(19), and showed a superoutburst with a precursor (Kapusta & Thorstensen 2006; Imada et al. 2009). Following Imada et al. (2009), we suggest that the radius of the accretion disk of OT J075418 should extend far beyond the 3 : 1 resonance radius, but not reach the tidal truncation radius, if a mass ratio of the system is small enough to provide a sufficient space between the 3 : 1 resonance and the tidal truncation radius.

As can be seen in the lightcurve, it took a relatively long time to change from the fading of a precursor outburst to the appearance of a superoutburst. It may be due to a long growth time of the 3 : 1 resonance because of its small mass ratio.

## 5.6 Number density problem of period bouncers

Now, we know four candidates for the period bouncer (OT J075418, SSS J122221, OT J230425, and OT J184228). To investigate whether our observations are capable of accounting for the missing population of period bouncers suggested by the evolutionary theory, we counted how many superoutbursts of SU UMa stars were observed. For the last five years, after the current project for observing SU UMa-type stars was undertaken the same as at present, we have observed about 291 superoutbursts in 248 SU UMa-type stars (Kato et al. 2010, 2012, 2013a, 2014a). The number of detected superoutbursts is unknown.[1]

The recurrence time of the superoutburst, $T_s$, is inversely proportional to mass-transfer rate $\dot{M}$ (Osaki 1995), and $\dot{M}$ is approximately proportional to $q^2$ in a short-period system evolved by gravitational radiation (Patterson 1998). We can estimate the parent population of the period bouncer from the statistics of recorded outbursts. Since many of SU UMa-type DNe have $T_s \sim 1$ yr, we can assume that many of them have been detected in a superoutburst for the last five years. If period bouncers have a recurrence time of $T_s$(PB), the detection probability of period bouncers can be estimated to be $f \times 5/T_s(\mathrm{PB})$, where $f$ stands for the fraction of time covered by surveys. If we conservatively assume $f \sim 0.1$–$0.5$, then we can estimate the ratio of parent populations of $N$(PB)/$N$(ordinary SU UMa-type) to be $\sim 4/248 \times 1/f \times T_s(\mathrm{PB})/5$.

There is a large uncertainty in $T_s$(PB). We can, however, estimate $T_s(\mathrm{PB}) > 5$ yr, since these objects were hardly detected in outbursts in the past CRTS and other surveys.[2] As to OT J230425, two outbursts have been detected by CRTS. One outburst was in 2006 December and the other was in 2011 January. It suggests that the recurrence time of the outbursts of OT J230425 is not as long as that of WZ Sge-type DNe. Therefore, it is possible that some candidates for the period bouncer have a higher mass-transfer rate than we expected and show outbursts more frequently than WZ Sge-type DNe. Three of the four candidates for the period bouncer, however, are WZ Sge-like stars. We assume that a majority of the candidates for the period bouncer are WZ Sge-like stars, and discuss the number density of period bouncers excluding such systems as OT J230425. We regard $N(\mathrm{PB}) = 3$ hereafter, excluding OT J230425.

If we assume that the mass-transfer is purely driven by the gravitational wave radiation, $\dot{M}(\mathrm{PB}) \sim 10^{-2}\,\dot{M}$(ordinary SU UMa-type) and $T_s$(PB) is expected to be $\sim 10^2$ yr. If we assume $T_s$(PB) is $\sim 10^1$ and $\sim 10^2$ yr and conservatively assume $f \sim 0.1$–$0.5$, we can obtain roughly $N(\mathrm{PB})/N(\mathrm{SU\,UMa}) \sim 0.048$–$2.4$. Considering the possibility of such period bouncers as OT J230425, the population of the period bouncer can be estimated to be larger. As mentioned in section 1, it was predicted that a majority of CVs [$\sim 70\%$ (Kolb 1993)] have passed

[1] There were systems of which superoutburst was detected but was not targets of time-series observations.

[2] Although a typical interval of observations in CRTS is 10 d, and there is a seasonal gap when the object is near the solar conjunction, we consider that many (fraction $f$) of the superoutbursts should have been recorded since WZ Sge-type DNe usually show a long-fading tail lasting several months. No previous outbursts in four systems suggest that $T_s$ for these systems is efficiently long.

the period bounce. On the contrary, few candidate for the period bouncer has been discovered from observations. We call the theoretically predicted population of the period bouncer the "missing population" of the period bouncer. Although the true recurrence time of candidates for the period bouncer should be confirmed by future observations, this ratio suggests a possibility that the period bouncers we have identified might account for the missing population of the period bouncer predicted by the evolutionary scenario. Thus we identify these WZ Sge-type objects with unusual outburst properties as the likely candidates for the hidden population of the terminal evolution of CVs.

Although we discussed photometric properties of the candidates for the period bouncer, Gänsicke et al. (2009) suggested their spectroscopic properties. They argued that SDSS CVs in the 80–86 min period spike showed spectra dominated by emission from the white dwarf with no spectroscopic signature from the companion star at optical wavelengths. These characteristics suggest that these systems have a very low accretion rate, and they are the most likely DNe with an extremely long recurrence time. It takes a long time to detect many candidates for the period bouncer in photometric observations on account of their long recurrence time. Spectroscopic studies of the four newly identified candidates are desired.

## 6 Summary

We report on photometric observations of two dwarf novae, OT J075418.7+381225 and OT J230425.8+062546, which showed superoutbursts in 2013 (OT J075418) and in 2011 (OT J230425). The results of the analysis of our data are summarized in table 5.

In OT J075418 and OT J230425, some peculiar properties that were similar to those of a likely candidate for the period bouncer (SSS J122221.7−311523) could be seen. These two DNe are likely candidates for the period bouncer. We then propose the general properties of candidates for the period bouncer below:

(i) They show a very long growing stage of superhumps (stage A) and a large period decrease of the stage A–B transition (∼ 1.5%). The long stage A, which reflects the slow evolution of the superhump, is due to the very small mass ratio of these objects.

(ii) The declining rates in the plateau phase in the superoutburst of these objects are lower than those of SU UMa-type DNe with a similar superhump period to these objects.

To investigate whether our observation is capable of accounting for the missing population of the period bouncer suggested by the evolutionary theory, we counted how many SU UMa stars showed superoutbursts. For the last five years, we have observed about 291 superoutbursts in 248 SU UMa-type stars, and the four likely candidates for the period bouncer have been suggested, including OT J075418 and OT J230425. Three of the four candidates were WZ Sge-like stars, and OT J230425 may have a shorter recurrence time than the others. We estimated the number density of the period bouncer from the stars excluding such systems as OT J230425. Although there is a large uncertainty in the recurrence time of period bouncers, we assumed that superoutbursts of the period bouncer were $10^1$–$10^2$ times less frequent than those of ordinary SU UMa-type DNe, according to the theoretical prediction. Under this assumption, we can obtain roughly $N$(PB)/$N$(SU UMa) ∼ 0.048–2.4. This ratio suggests a probability that the period bouncers we have identified might account for the missing population of the period bouncers predicted by the evolutionary scenario.

**Table 5.** Results of the analysis of OT J075418 and OT J230425.

| | OT J075418 | OT J230425 |
|---|---|---|
| Mean period* | 0.0722403(26) | 0.067317(35) |
| Stage A† | 0.072218(3) | 0.067245(17) |
| | (56328–56341) | (55563–55572) |
| Stage B‡ | 0.070758(6) | 0.066351(12) |
| | (56345–56355) | (55571–55585) |
| Fading rate§ | 0.0189(3) | 0.0340(4) |

*Mean period of the all superhumps in units of d.
†Stage A superhump period in units of d. The interval used for determining the period is in parentheses. BJD−2400000.
‡Stage B superhump period in units of d. The interval used determin the period in parentheses. BJD−2400000.
§In units of mag $d^{-1}$.

## Acknowledgments

This work was supported by a Grant-in-Aid "Initiative for High-Dimensional Data-Driven Science through Deepening of Sparse Modeling" from the Ministry of Education, Culture, Sports, Science and Technology (MEXT) of Japan. We are grateful to many amateur observers for providing a lot of data used in this research.

## References

Bailey, J. 1979, MNRAS, 189, 41P
Cleveland, W. S. 1979, J. Amer. Statistical Assoc., 74, 829
Downes, R. A. 1990, AJ, 99, 339
Drake, A. J., et al. 2009, ApJ, 696, 870
Fernie, J. D. 1989, PASP, 101, 225
Gänsicke, B. T., et al. 2009, MNRAS, 397, 2170
Hiroi, K., et al. 2009, PASJ, 61, 697
Imada, A., et al. 2009, PASJ, 61, L17
Kapusta, A. B., & Thorstensen, J. R. 2006, PASP, 118, 1119

Kato, T. 2002, PASJ, 54, L11
Kato, T., et al. 2009, PASJ, 61, S395
Kato, T., et al. 2010, PASJ, 62, 1525
Kato, T., et al. 2012, PASJ, 64, 21
Kato, T., et al. 2013a, PASJ, 65, 23
Kato, T., et al. 2014a, PASJ, 66, 30
Kato, T., et al. 2014b, PASJ, 66, L7
Kato, T., & Maehara, H. 2013, PASJ, 65, 76
Kato, T., Monard, B., Hambsch, F.-J., Kiyota, S., & Maehara, H. 2013b, PASJ, 65, L11
Kato, T., & Osaki, Y. 2013, PASJ, 65, 115
Kato, T., Sekine, Y., & Hirata, R. 2001, PASJ, 53, 1191
Kato, T., & Uemura, M. 2012, PASJ, 64, 122
Knigge, C., Baraffe, I., & Patterson, J. 2011, ApJS, 194, 28
Kolb, U. 1993, A&A, 271, 149
Littlefair, S. P., Dhillon, V. S., Marsh, T. R., Gänsicke, B. T., Southworth, J., Baraffe, I., Watson, C. A., & Copperwheat, C. 2008, MNRAS, 388, 1582
Littlefair, S. P., Dhillon, V. S., Marsh, T. R., Gänsicke, B. T., Southworth, J., & Watson, C. A. 2006, Science, 314, 1578
Lubow, S. H. 1991, ApJ, 381, 259
Lubow, S. H. 1992, ApJ, 398, 525
Murray, J. R. 2000, MNRAS, 314, L1
Nakano, S., Nishimura, H., Kadota, K., & Yusa, T. 2011, Cent. Bur. Electron. Telegrams, 2616
Nakata, C., et al. 2013, PASJ, 65, 117
Nogami, D., Kato, T., Baba, H., Matsumoto, K., Arimoto, J., Tanabe, K., & Ishikawa, K. 1997, ApJ, 490, 840
Osaki, Y. 1989, PASJ, 41, 1005
Osaki, Y. 1995, PASJ, 47, 47
Osaki, Y., & Kato, T. 2013, PASJ, 65, 50
Osaki, Y., & Meyer, F. 2003, A&A, 401, 325
Patterson, J. 1998, PASP, 110, 1132
Patterson, J. 2011, MNRAS, 411, 2695
Patterson, J., et al. 1998, PASP, 110, 1290
Stellingwerf, R. F. 1978, ApJ, 224, 953